17th World Conference on Earthquake Engineering, 17WCEE
Sendai, Japan - September 13th to 18th 2020

SCENARIO-BASED PERFORMANCE ASSESSMENT OF DAMS USING STOCHASTIC GROUND MOTION SIMULATIONS

M.A. Hariri-Ardebili[1], S. Rezaeian[2]

[1] *Research Associate, National Institute of Standards and Technology (NIST), amin.hariri@nist.gov*
[2] *Research Structural Engineer, U.S. Geological Survey (USGS), srezaeian@usgs.gov*

Abstract

Advanced risk analysis of engineering structures requires nonlinear analyses as well as accurate approximation of both aleatory and epistemic uncertainties. A great source of uncertainty comes from the input seismic excitation, which highly affects the results of probabilistic seismic performance assessment of dams. In this study, we investigate the effects of uncertainties in input ground motion excitations on seismic fragility analyses of concrete dams by performing scenario-based performance assessment recommended by ATC-58 guidelines.

Due to the scarcity of recorded ground motions, stochastic ground motion simulation methods can be used to obtain the necessary input excitations and good approximations of ground motion variabilities. This study utilizes the Rezaeian and Der Kiureghian [14] stochastic simulation model. Different seismic hazard scenarios (each defined by an earthquake magnitude, source-to-site distance, and local soil conditions) are considered in a parametric study to represent uncertainty in scenario selection and capture the record-to-record variability of ground motions. A detailed finite element model of a dam-foundation coupled system is developed, where the nonlinearity is originated from an advanced zero-thickness interface joint element between the concrete and rock. Fragility curves and surfaces are computed based on the cloud analysis technique, while different damage measures and limit state functions are considered.

A variety of intensity measure (IM) parameters (e.g., peak ground acceleration, first-mode spectral acceleration, and Arias intensity) are extracted from the simulated ground motion signals in order to determine a set of optimal IMs. These optimal IMs are determined by employing a systematic procedure based on criteria such as efficiency, practicality, proficiency, sufficiency, and hazard compatibility [20]. The procedure is based on developing a probabilistic seismic demand model (PSDM), using the results from structural analyses. A linear regression model is fitted to the discrete data points in the logarithmic scale, and its constants are used for optimal IM selection. Moreover, the logarithmic standard deviation of the engineering demand parameters conditioned on the IM is used to rank the efficiency of the IMs.

It is found that in any probabilistic seismic hazard and risk analyses, the resulting fragility curves are highly sensitive to several factors including the initial record selection from different earthquake scenarios and different methods for calculating fragility curves. The sensitivity to different engineering demand parameters is found to be relatively minor.

Keywords: Uncertainty, Fragility, Seismic, Stochastic, Concrete Dam

1. Introduction

Quantification of seismic uncertainty in performance assessment of geo-structures (e.g., concrete and embankment dams, quarry and gravity retaining walls) is a critical step towards risk management. Performance-based earthquake engineering (PBEE) is an analysis method which accounts for different types of uncertainties and presents the results in a language which is understandable for engineers (i.e., fragility functions) and stakeholders (i.e., loss functions) [1].

In the next-generation PBEE methodology [1], seismic performance assessment is broken down into four primary steps: 1) ground motion hazard characterization, 2) structural response analysis, 3) damage analysis, and 4) loss assessment. Each step is presented in the form of generalized variables including the intensity measure (IM), engineering demand parameter (EDP), damage measure (DM), and decision variable (DV). This process can be expressed based on the total probability theorem [1]:

$$g\left[\mathrm{DV}|\mathrm{D}\right]=\iiint p\left[\mathrm{DV}|\mathrm{DM},\mathrm{D}\right]p\left[\mathrm{DM}|\mathrm{EDP},\mathrm{D}\right]p\left[\mathrm{EDP}|\mathrm{IM},\mathrm{D}\right]g\left[\mathrm{IM}|\mathrm{D}\right]d\mathrm{IM}.d\mathrm{EDP}.d\mathrm{DM} \quad (1)$$

where p[X|Y] denotes the complementary cumulative distribution function (CDF) of X conditioned on Y, g[X|Y] denotes the mean annual occurrence rate of X given Y, and D denotes the facility location.

Applied Technology Council (ATC) [2] introduced three types of performance assessments (all in the context of next-generation PBEE): 1) intensity-based (where the intensity of ground motion should be specified in addition to the design scenario), 2) scenario-based (where only the design scenario needs to be specified), and 3) time-based (where all the possible design scenarios and their probabilities of occurrence are taken into account). In this paper, scenario-based performance assessment (SBPA) is adopted for fragility assessment of geo-structures. SBPA evaluates a structure's performance assuming that it is subjected to the effects of a specific magnitude earthquake occurring at a specific location relative to the structure site. This approach can be very useful for decision makers with structures located close to one or more known active faults [2].

These three techniques (and specifically SBPA) require an appropriate suite of ground motion time-series to be used in numerical simulations. The first (and probably the best) source is to select a group of recorded ground motions that are only slightly modified (e.g., scaled). Ground motion selection [3, 4, 5] and scaling [6, 7] have a long history in earthquake engineering and most of the times are combined to obtain a suite of ground motion time-series.

In the field of dam engineering, application of real ground motions (including their selection and scaling) is state-of-the-practice. Some of the International Commission on Large Dams (ICOLD) bulletins discuss very general concepts on how to select the most appropriate ground motion records for dam analysis [8]. Although there is no official recommendation on selection and scaling of the ground motion records for probabilistic assessment of dams, nearly all current applications have adopted (at some level) the state-of-the-practice techniques [9].

However, all PBEE-rooted probabilistic methods suffer from having a limited number of recorded ground motions (which typically cover a narrow and discrete range of seismic hazard) and may necessitate simulation of extra ground motion records. This field (i.e., ground motion simulation) is nearly untouched in dam engineering for four main reasons: 1) the state-of-the-practice in dam engineering is deterministic evaluation, which requires relatively few ground motions, 2) there is no official legislation on the application of probabilistic techniques, 3) limited research on probabilistic assessment of dams requires a larger set of ground motions [9], and 4) the current focus of the dam research community is to develop the “best practice” seismic dam-foundation-reservoir analysis which properly matches the recorded dam response [10-13], taking the spotlight away from advancing probabilistic analyses. Given the current gap in dam engineering, there is an urgent need for pilot research on the application of simulated ground motions, as opposed to selection and scaling methods, to further PBEE-rooted probabilistic methods.

Most recent ground motion simulation techniques are capable of generating acceleration time-series based on a particular seismic hazard scenario, which makes them an excellent option for use in SBPA [14, 15]. In general, these techniques can be divided into two groups [16, 17]:

- Physics-based models simulate the ground motion by explicitly modeling the fault rupture, wave propagation, and near-surface site amplification. The models require relatively precise seismological and geophysical information about each of these three elements to provide good estimation of real ground motions. This approach is, in general, expensive to implement and not very accurate for high-frequency motions [18].

- Stochastic models directly simulate the ground motion time-series and are empirically calibrated based on the existing dataset. This approach is, in general, computationally inexpensive. Stochastic models can be constructed using one of the following methods [14]: 1) passing white noise through a filter, 2) passing a train of Poisson pulses through a linear filter, 3) applying autoregressive moving average modeling, and 4) using evolutionary spectral modeling approaches. To obtain a good estimation of real ground motion time-series for nonlinear analyses, both the temporal non-stationarity (the amplitude changes with time) and the spectral non-stationarity (the frequency changes with time) should be accounted for in the model.

Furthermore, the application of simulated ground motions in probabilistic analyses has been shown to be promising. For example, [19] studied the impact of record scaling on the overall bias in nonlinear single-degree-of-freedom (SDOF) and multi-degree-of-freedom (MDOF) systems. Two large sets of real and stochastic motions were gathered (over 1,000 records). They found that the ground motion bias is similar for the recorded and synthetic motions.

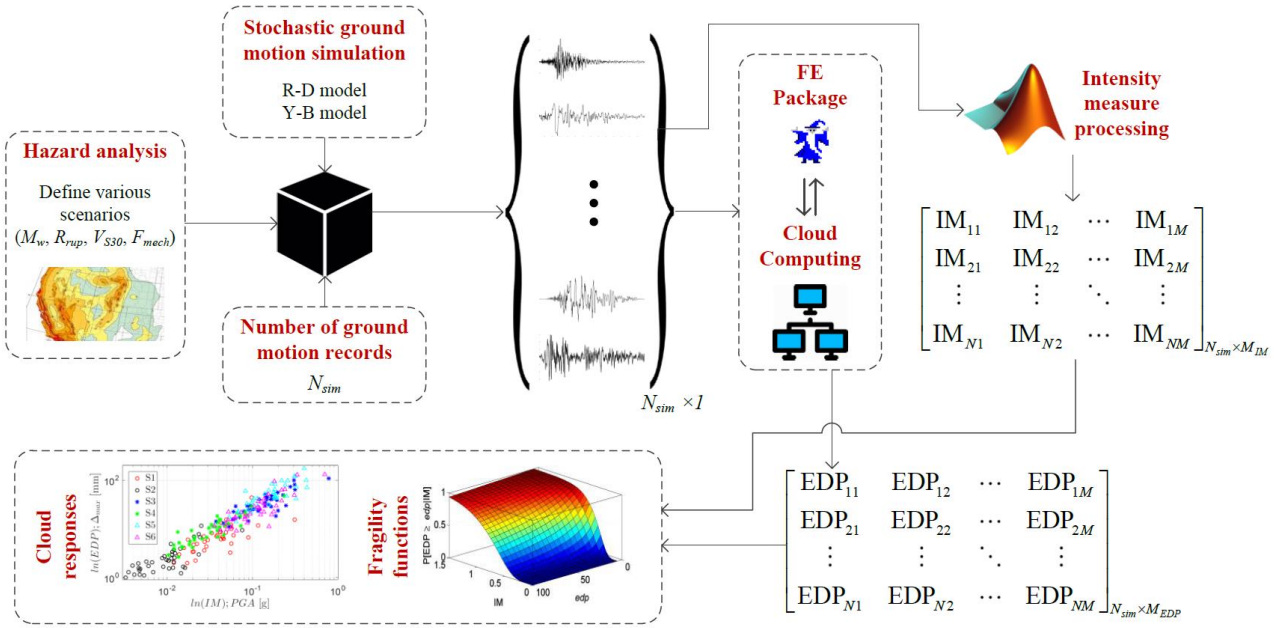

Fig. 1 – The general algorithm for the proposed probabilistic seismic response analysis with stochastic ground motion records

This paper combines the SBPA approach with simulated ground motions for efficient fragility analysis of concrete dams. Motivation for this study is due to a dearth of real ground motion recordings for SBPA for the site of the presented case study dam [20]. This paper has several major contributions. To the best of authors' knowledge, it is the first application of SBPA on dams, as well as the first application of stochastic

ground motion simulations in cloud analysis of geo-structures. To address epistemic uncertainty in ground motion simulation procedures, we considered two stochastic models to understand the model-to-model variability and present only one simulation method due to paper length limitations. Structural analyses are performed for a particular case study for different seismic hazard scenarios, the fragility curves and surfaces are then derived and compared for each scenario. Finally, a discussion is provided on the optimal IM parameters based on the stochastic ground motion model; a topic that has already been addressed for dams using real ground motion recordings in [20]. A schematic flowchart of the workflow is shown in Fig.1. It combines the identified seismic hazard scenarios with ground motion simulation techniques to provide probabilistic input for the finite element (FE) modeling of dams. The post-processed outputs (i.e., EDPs) and inputs (i.e., IMs) are then used to develop comparative cloud data and fragility functions.

2. Underpinning Theories

2.1. Rezaeian and Der Kiureghian Stochastic Ground Motion Simulation Model

Rezaeian and Der Kiureghian [14] developed a fully non-stationary stochastic ground motion model based on a modulated filtered white-noise process with time-varying parameters. In this model, the temporal and spectral non-stationary characteristics are completely decoupled, which facilitates identification of the model parameters. The model has a small number of parameters with physical interpretations. Details of the model can be found in [14, 17].

The ground motion model parameter vector can be summarized as $\theta = \left\{ I_A, D_{5-95}, t_{mid}, \omega_{mid}, \omega', \zeta_f \right\}$. Predictive relationships have been developed for each model parameter by fitting the stochastic model to a subset of the Next Generation Attenuation (NGA) strong motion database. These predictive models describe θ in terms of the following earthquake and site characteristics: 1) moment magnitude (M_w), 2) closest distance to rupture (R_{rup}) in [km], 3) shear wave velocity of the top 30 m of soil (V_{S30}) in [m/s], and 4) fault mechanism (F_{mech}), either strike-slip or reverse. The empirical equations take the following generic form:

$$\Phi^{-1}\left[F_\theta(\theta)\right] = \mu\left(M_\omega, R_{rup}, V_{S30}, F_{mech}, c\right) + \eta + \sigma \tag{2}$$

where θ is a model parameter, $\Phi[.]$ is the standard Gaussian cumulative distribution function (CDF) and F_θ is the CDF of θ (which is empirically determined). Subsequently, $\Phi^{-1}\left[F_\theta(\theta)\right]$ transforms a model parameter from the physical space to the standard normal space. μ is the predicted mean as a function of the earthquake and site characteristics (i.e., earthquake hazard scenario) and *c* represents the vector of regression coefficients. Moreover, η and σ are normally distributed zero-mean random variables and refer to the inter-event and the intra-event errors, respectively. The regression coefficients, the variances of the error terms, and the correlations between the model parameters can be found in [14] for shallow crustal earthquakes and in [17] for stable continental earthquakes.

2.2. Fragility Function

A probabilistic seismic demand model (PSDM) is a conditional probability statement that expresses the probability that a system or any of the structural components experience a certain level of demand (D) for a given intensity measure (IM) level, *P*[D|IM]. Results of a PSDM (using multiple nonlinear analysis in the context of cloud analysis – CLA) can be presented in terms of a fragility function. Cloud analysis is a wide-range nonlinear analysis technique in which the structure is subjected to a set of un-scaled ground motions. The ground motions are selected (or generated) based on a particular earthquake scenario. The extreme EDPs are then extracted and plotted versus the ground motion IMs, which forms a so-called “cloud response.”

CLA results can then be used to develop a fragility function assuming that the conditional seismic demand has a lognormal distribution [21]:

$$P\left[\text{EDP} \geq edp \mid \text{IM}\right] = 1 - \Phi\left(\frac{\ln(edp) - \ln(\eta_{\text{EDP|IM}})}{\beta_{\text{EDP|IM}}}\right) \tag{3}$$

where $\eta_{\text{EDP|IM}}$ and $\beta_{\text{EDP|IM}}$ are median and logarithmic standard deviation of the EDP conditioned on the IM, respectively.

Eq. (3) is used in the case that all nonlinear analyses converge and the extreme EDPs are less than failure capacity. Should there be any numerical failures in the analyses, Eq. (3) has to be altered as in [22]:

$$\begin{aligned} P\left[\text{EDP} \geq edp \mid \text{IM}\right] = {} & P\left[\text{EDP} \geq edp \mid \text{IM,NLg}\right].\left(1 - P\left[\text{Lg} \mid \text{IM}\right]\right) \\ & + P\left[\text{EDP} \geq edp \mid \text{IM,Lg}\right].\left(P\left[\text{Lg} \mid \text{IM}\right]\right) \end{aligned} \tag{4}$$

where $P\left[\text{Lg} \mid \text{IM}\right]$ is the probability of having "very large" (Lg) EDP for a given IM. $P\left[\text{EDP} \geq edp \mid \text{IM,Lg}\right] = 1$ (i.e., in the case of global failure, any pre-defined limit state (LS) is certainly exceeded), and $P\left[\text{EDP} \geq edp \mid \text{IM,NLg}\right]$ is the fragility function given "not very large" (NLg) EDP and is constructed by replacing IM in Eq. (3) with IM,NLg.

2.3. Optimal Intensity Measure Parameter

Selection of the optimal IM parameter for structures [23, 24] as well as concrete dams [20] should be based on the following criteria:

- Efficiency: An efficient IM reduces the EDP variability for a given IM. It corresponds to smaller $\beta_{\text{EDP|IM}}$ in Eq. (3).
- Practicality: It is an indicator of the correlation between an IM and the EDP. Higher slope (*b* value) in the following equation being indicative of increased practicality.

$$\ln\left(\eta_{\text{EDP|IM}}\left(\text{IM}\right)\right) = b.\ln \text{IM} + \ln a \tag{5}$$

- Proficiency: It is a composite measure of efficiency and practicality. A more proficient IM would have lower modified dispersion, $\zeta = \beta_{\text{EDP|IM}} / b$.
- Sufficiency: The conditional probability of EDP on a sufficient IM should be independent from the seismic hazard parameters such as M_w, R_{rup}, ε (variation) and T_p (pulse period) as defined in [24]:

$$P\left[\text{EDP} \geq edp \mid \text{IM}\right] \cong P\left[\text{EDP} \geq edp \mid \text{IM},M_{\omega},R_{rup},\varepsilon,T_p\right] \tag{6}$$

  Note that sufficiency is not fully controlled for SBPA as all the records are selected based on a particular earthquake scenario.
- Hazard compatibility: The selected optimal IM should be captured through the hazard curves [25]. Example of hazard-compatible IMs are PGA and S_a(T).

3. Numerical Example

A gravity dam is selected as the case study in this paper. The height of the dam is 121.92 m, thickness at the base and the crest are 95.81 and 9.75 m, respectively. Upstream and downstream face slopes are 0.05 and 0.78, respectively. Four-node and three-node plain strain elements are used for modeling the dam body and the foundation, Fig. 2. The nonlinearity in the coupled system is considered by modeling the dam-foundation interface joints using zero-thickness interface elements [26]. There are about 20 elements along the base joint which provide acceptable accuracy of joint failure. The finite element code "Merlin" is used for dynamic analyses [27].

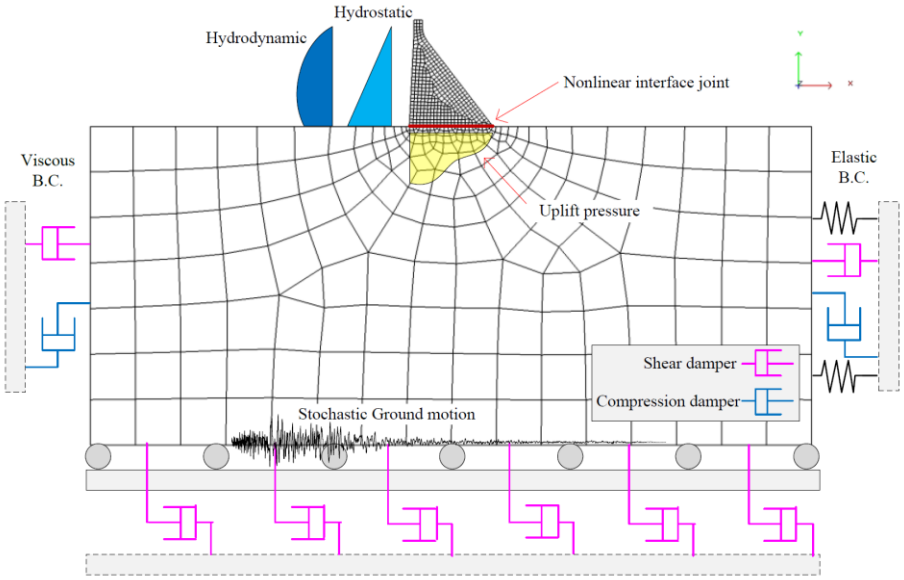

Fig. 2 – FEM-based model description (loads and boundary conditions)

The applied loads on the system are: 1) self-weight, 2) hydrostatic pressure, 3) dynamic uplift which is automatically updated with crack propagation, and 4) seismic loads (only the horizontal component is applied). The viscous boundary condition (B.C.) is modeled on the foundation far-end edges to absorb the outgoing (S- and P-) waves. Furthermore, the elastic boundary is modeled on one side of the foundation to prevent the rigid body motion. Dynamic analysis is "restarted" (only displacement is reset to zero without altering the initial stress state) after the initial static one [27]. Damping is modeled based on mass- and stiffness-proportional Rayleigh coefficients assuming a 5% of critical damping for the system. The coupled system fundamental period is estimated to be 0.44 s.

4. Results

4.1. Parametric Study on Earthquake Scenarios

In the following, six different seismic hazard scenarios are defined (Table 1) and used to examine the sensitivity of the stochastic ground motion model to different scenarios, and the variation of responses. In the first four scenarios, we only vary M_w and R_{rup}, while the shear wave velocity V_{S30} is constant. In the last two scenarios, V_{S30} is also a variable. Among these six scenarios, S3 is considered the pilot scenario (a common magnitude and distance in seismic design) and the variations of results generated by the other scenarios are presented with respect to S3.

For each of the six scenarios, 40 ground motion time-series are simulated. Thus, overall 6×40 = 240 time-series are generated. Acceleration response spectra of these 240 time-series are shown in Fig. 3 along

with their mean and mean ± one standard deviation. Qualitatively, one can recognize the higher spectra for the earthquake scenarios with larger M_w and smaller R_{rup} (i.e., S3, S5, and S6). Moreover, in order to have a better understanding about the time-history nature of these stochastic motions, the "double normalized Arias intensity", I_A plots, where both time and I_A are normalized to unity (and shown as 100% maximum), are also illustrated in Fig. 3.

Table 1 - Earthquake scenarios for performance-based assessment

Scenarios	M_w	R_{rup}	V_{S30}	F_{mech}
S1	5.5	20	760	Strike-slip
S2	5.5	100	760	Strike-slip
S3	7.0	20	760	Strike-slip
S4	7.0	100	760	Strike-slip
S5	7.0	20	380	Strike-slip
S6	7.0	20	1140	Strike-slip

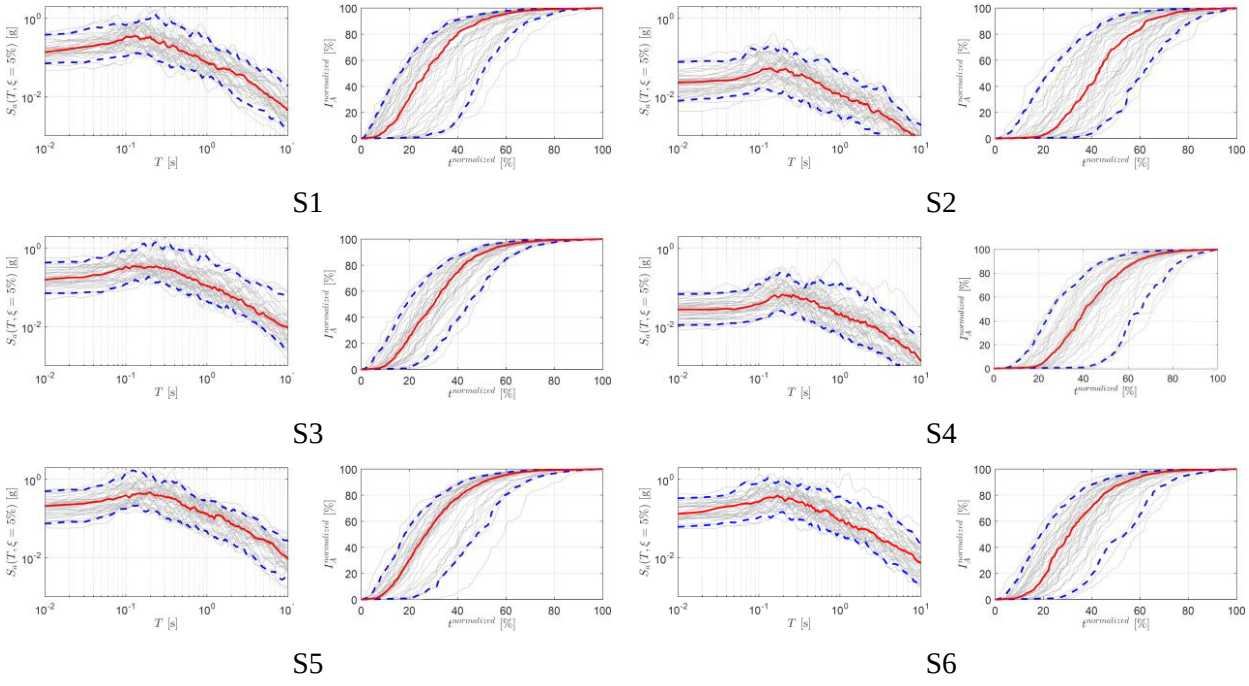

Fig. 3 – Acceleration response spectra and normalized Arias intensity of the simulated ground motions

4.2. Structural Responses

As previously mentioned, the cloud analysis technique is used in this paper, and the resulting EDPs are shown versus the IM parameters in Fig. 4. Here, we use maximum crest displacement, Δ^H_{max}, as the EDP and three IM parameters: PGA, S_a(T1), and I_A. There are several observations in this figure:

- Results show a linear trend in the logarithmic scale.

- Among the three selected IM parameters, S_a(T1) has the least and PGA has the most dispersion.
- As expected, among the six scenarios, S2 has the smallest EDPs (since it has smaller M_w and larger R_{rup}), while S3, S5, and S6 have the highest EDPs (differences discussed later).

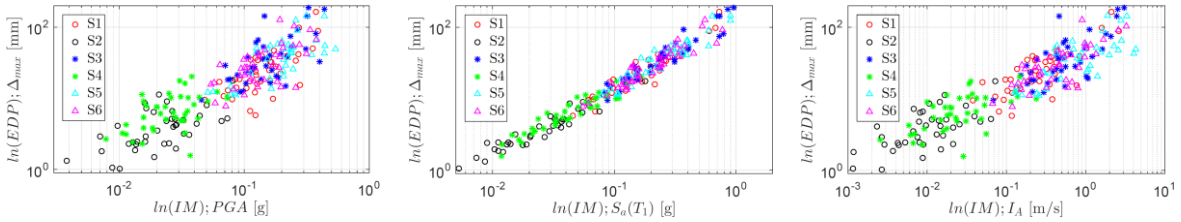

Fig. 4 – Cloud analysis results in logarithmic scale with crest displacement as EDP and three different IM parameters

Fig. 5 compares the different scenarios for all four influencing EDPs: the maximum crest displacement, Δ^H_{max}, the maximum crest displacement normalized base crack length, L_{cr}, maximum base joint opening, $\Delta^{opening}$, and maximum base joint sliding, $\Delta^{sliding}$. The major observation is that the general trend of the four EDPs subjected to the six different scenarios are similar: for all the EDPs, some scenarios, e.g., S3 and S5 lead to higher dispersion, while some others, e.g., S2 and S4 show minimum values. This means that the results are not very sensitive to the selected EDPs.

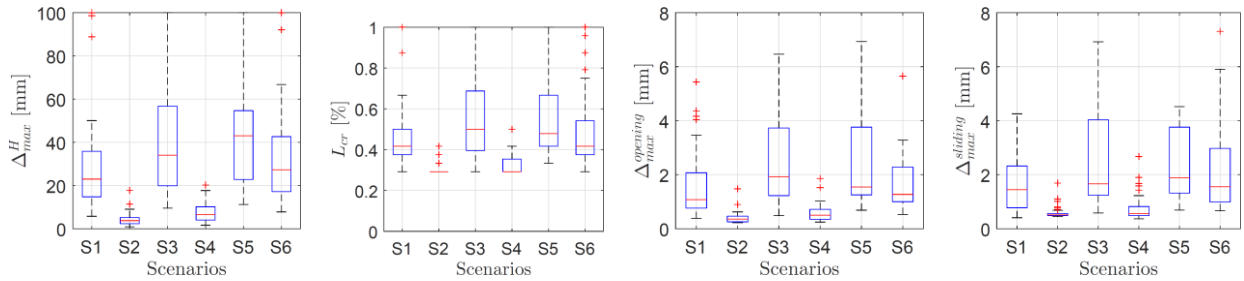

Fig. 5 – Statistics of the engineering demand parameters; Note: boxplots show interquartile range (IQR), with median; mínimum/maximum values times 1.5 IQR; outliers as individual points

4.3. Optimal Intensity Measure

Fig. 6 illustrates the selection of the optimal IM parameter based on different scenarios. The IMs considered in this figure are: ASI (acceleration spectrum intensity), VSI (velocity spectrum intensity), S_a(T1) defined as the first-mode spectral acceleration, S_v(T1) defined as the first-mode spectral velocity, PGA (peak ground acceleration), PGV (peak ground velocity), RMSa (root-mean-square of acceleration), RMSv (root-mean-square of velocity), I_A (Arias intensity), SED (specific energy density), and CAV (cumulative absolute velocity) [28]. The major observations are:

- Practicality: Higher *b* means higher practicality. High-practicality IMs for each scenario are:
  - S1: CAV, ASI, PGV
  - S2: PGV, CAV, ASI
  - S3: ASI, VSI, S_v(T1)
  - S4: S_v(T1), ASI, CAV
  - S5: VSI, PGV, CAV

  - S6: CAV, S_v(T1), ASI
  - Over all six scenarios, the top priorities are: CAV, ASI, PGV, and S_v(T1).
- Efficiency: Smaller β means higher efficiency. High-priority IMs for each scenario are:
  - S1: S_v(T1), S_a(T1), ASI
  - S2: S_v(T1), S_a(T1), VSI
  - S3: S_a(T1), S_v(T1), VSI
  - S4: S_a(S1), S_v(T1), VSI
  - S5: S_v(T1), S_a(T1), VSI
  - S6: S_v(T1), S_a(T1), v_{RMS}
  - Over all six scenarios, the top priorities are: S_v(T1), S_a(T1), and VSI.
- Proficiency: Smaller ζ means higher proficiency. High-priority IMs for each scenario are:
  - S1: S_v(T1), S_a(T1), ASI
  - S2: S_v(T1), S_a(T1), VSI
  - S3: S_a(T1), S_v(T1), VSI
  - S4: S_a(T1), S_v(T1), VSI
  - S5: VSI, S_v(T1), S_a(T1)
  - S6: S_v(T1), S_a(T1), v_{RMS}
  - Over all six scenarios, the top priorities are: S_v(T1), S_a(T1), and VSI.

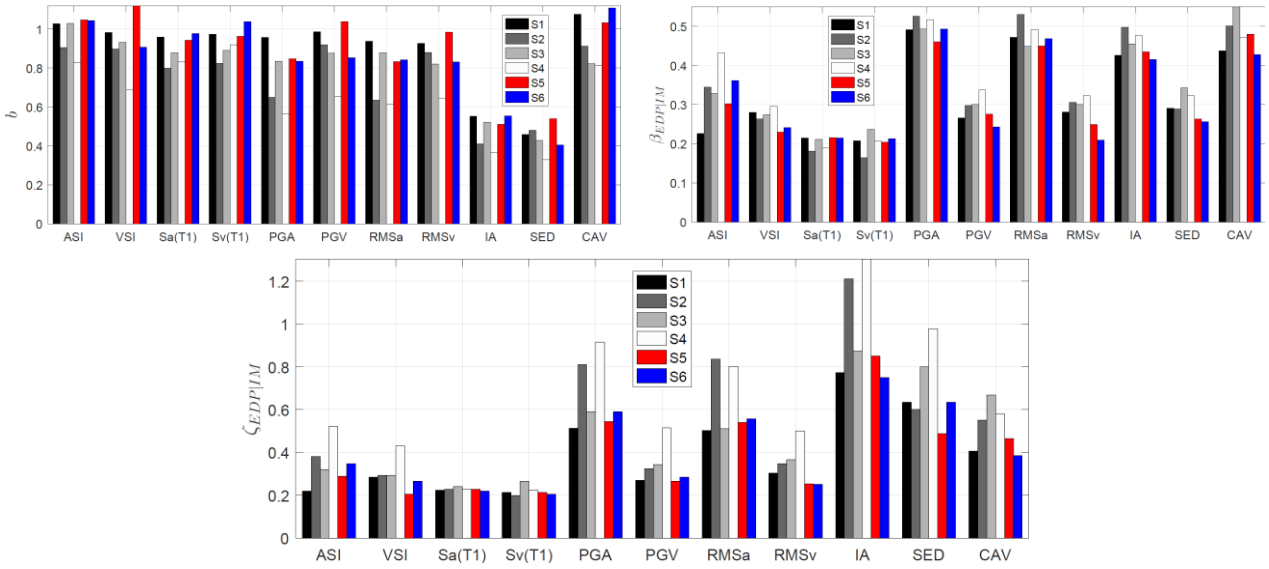

Fig. 6 – Evaluating optimality of different IM parameters based on crest displacement response

4.4. Fragility Assessment

Based on the previous section, S_v(T1) and S_a(T1) appear to be the optimal IM parameters in nearly all scenarios. Thus, it is reasonable to develop the fragility functions based on these two parameters. However, S_a(T1) is hazard compatible as well. Therefore, we adopt only S_a(T1) as the IM parameter in our fragility curves. Fragility curves can be derived based on one of the following cases:

- Case 1: $P\left[\text{EDP} \geq edp \mid \text{IM}\right]$ is determined from the complete data set, Eq. (3).
- Case 2: The large (or failed) data points are bounded to a user-defined limit (usually the largest non-collapse data) and $P\left[\text{EDP} \geq edp \mid \text{IM}\right]$ is determined using Eq. (3).

- Case 3: The large data points are not considered, and only $P\left[\text{EDP} \geq edp \mid \text{IM,NLg}\right]$ is calculated.
- Case 4: All the large and not large data points are used, Eq. (4).

Fig. 7 shows the fragility curves for the six scenarios and above four cases (total of 24 curves). Since the intensity of the stochastic ground motions is different for various scenarios, three different target *edps* are assumed to derive the fragility curves. S3, S5 and S6 are high-intensity scenarios, thus, the target *edp* = 0.05% H_{dam} (height of the dam) is used. S1 is a moderate-intensity scenario, and therefore the target *edp* = 0.03% H_{dam} is used. Finally, S2 and S4 are low-intensity scenarios and the target *edp* = 0.01% H_{dam} is used. The major observations are:

- Since NLg data either do not exist or are very rare in S2 and S4, the four fragility curves associated with the four cases are identical for these two scenarios.
- For the S1 scenario, the four fragility curves are nearly identical. S_a(T1) associated with 50% probability of exceedance is 0.27g.
- Fragility curves associated with the four cases are different from each other in S3, S5, and S6. This proves that the Lg data have some level of contribution in ultimate fragility functions. Thus, one may regard Case-4 as a final product of the fragility analysis.
- Special attention should be given to the S6 scenario. In general, Case-4 is built on Case-3. For S6, the curve associated with Case-4 is diverted from Case-3 for S_a (T1) > 0.5g. This shows that the majority, if not all, of the Lg data occur when S_a (T1) > 0.5g.

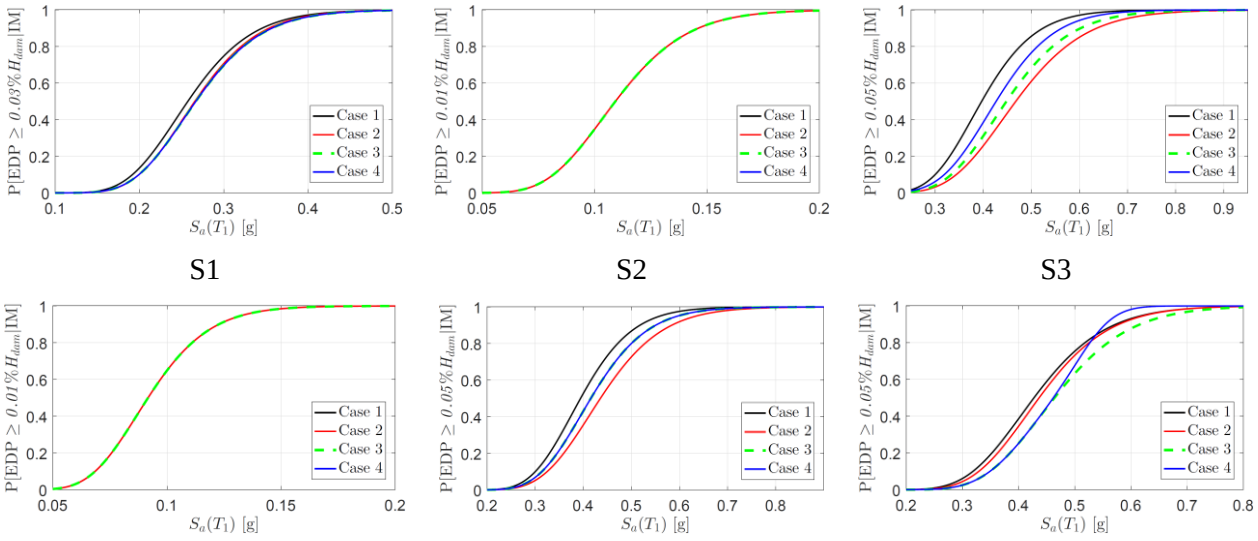

Fig. 7 – Displacement-based fragility curves with different formulations

5. Conclusions

This paper presented the results of nonlinear seismic analysis of a concrete dam using a stochastic ground motion simulation model. The times series are generated based on a scenario-based performance assessment. In this technique, only the earthquake magnitude, source-to-site distance, shear wave velocity and the fault mechanism are the input parameters. This paper included multiple objectives: 1) utilization of stochastically simulated time-series in dynamic analysis of geo-structures, 2) development of cloud analysis for geo-structures, 3) determination of optimal intensity measure parameters, 4) derivation of fragility curves based

on different assumptions, demand parameters, and limit states. Comprehensive discussions on the results in each section focused on the sensitivity of the results to different modeling elements, from ground motion time-series variabilities to hazard scenario selection, different engineering demand parameters, and different approaches to calculating fragilities.

4. Acknowledgements

This research was partially supported by the U.S. Geological Survey (USGS) and the National Institute of Standards and Technology (NIST). This support and the reviews provided by these agencies are gratefully acknowledged. The opinions and findings in this paper are those of the authors, supported by the USGS, and do not necessarily reflect the views of other sponsoring agencies.

6. References

[1] Porter K (2003): An overview of PEER's performance-based earthquake engineering methodology. San Francisco, CA.

[2] Applied Technology Council (2012): Seismic performance assessment of buildings, Volume 1: Methodology. ATC-58-1: Federal Emergency Management Agency Redwood City, CA.

[3] Baker Jack W, Allin Cornell C (2006): Spectral shape, epsilon and record selection. *Earthquake Engineering & Structural Dynamics*, 35(9), 1077–1095.

[4] Bradley Brendon A (2010): A generalized conditional intensity measure approach and holistic ground-motion selection. *Earthquake Engineering & Structural Dynamics*, 39(12), 1321–1342.

[5] Kwong N Simon, Chopra Anil K, McGuire Robin K (2015): A framework for the evaluation of ground motion selection and modification procedures. *Earthquake Engineering & Structural Dynamics*, 44(5), 795–815.

[6] Naeim F, Alimoradi A, Pezeshk S (2004): Selection and scaling of ground motion time histories for structural design using genetic algorithms. *Earthquake Spectra*, 20, 413–426.

[7] Huang YN, Whitaker AS, Luco N, Hamburger R (2011): Scaling earthquake ground motions for performance-based assessment of buildings. *Journal of Structural Engineering*, 137(3), 311–321.

[8] ICOLD (2016). Selecting seismic parameters for large dams, Guidelines, Bulletin 148 (Revision of Bulletin 72). : International Commission on Large Dams. Paris, France.

[9] Hariri-Ardebili MA, Saouma V E (2016): Seismic Fragility Analysis of Concrete Dams: A State-of-the-Art Review. *Engineering Structures*, 128, 374–399.

[10] Proceedings of the 12th ICOLD International BenchmarkWorkshop. In: Zenz G., Goldgruber M., eds. Numerical Analysis of Dams, :1–426ATCOLD, Austrian National Committee on Large Dams; 2014; Graz, Austria

[11] Proceedings of the 13th ICOLD International Benchmark Workshop. In: Gunn R.M., Balissat M., Manso P., Mouvet L., Schleiss A., eds. Numerical Analysis of Dams, :1–418SwissCOD, Swiss Committee on Dams; 2016; Lausanne, Switzerland.

[12] Proceedings of the 14th ICOLD International Benchmark Workshop. In: Malm R., Hassanzadeh M., Hellgren R., eds. Numerical Analysis of Dams, :1–722ATCOLD, Austrian National Committee on Large Dams; 2018; Stockholm, Sweeden.

[13] Salamon Jerzy W (2018): Evaluation of Numerical Models and Input Parameters in the Analysis of Concrete Dams. DSO-19-13: U.S. Bureau of Reclamation, Denver, Colorado.

[14] Rezaeian Sanaz, Der Kiureghian Armen (2010): Simulation of synthetic ground motions for specified earthquake and site characteristics. *Earthquake Engineering & Structural Dynamics*, 39(10), 1155–1180.

[15] Yamamoto Yoshifumi, Baker JackW (2013): Stochastic model for earthquake ground motion using wavelet packets. *Bulletin of the Seismological Society of America*, 103(6), 3044–3056.

[16] Yamamoto Y (2011): Stochastic model for earthquake ground motion using wavelet packets. *PhD thesis*, Stanford University, Stanford Palo-Alto, CA.

[17] Rezaeian Sanaz, Sun Xiaodan (2014): Stochastic ground motion simulation. *Springer*, Berlin, Heidelberg, 1-33.

[18] Taborda Ricardo, Roten Daniel (2014): Physics-based ground-motion simulation, *Springer*, Berlin, Heidelberg, 1–33.

[19] Mehdizadeh Mohammad, Mackie Kevin R, Nielson Bryant G (2017): Scaling Bias and Record Selection for Quantifying Seismic Structural Demand. *Journal of Structural Engineering*, 143(9), 04017117.

[20] Hariri-Ardebili MA, Saouma V (2016): Probabilistic seismic demand model and optimal intensity measure for concrete dams. *Structural Safety*, 59, 67–85.

[21] Cornell AC, Jalayer F, Hamburger RO (2002): Probabilistic basis for 2000 SAC federal emergency management agency steel moment frame guidelines. *Journal of Structural Engineering*, 128, 526–532.

[22] Jalayer F, Franchin P, Pinto PE (2007): A scalar damage measure for seismic reliability analysis of RC frames. *Earthquake Engineering and Structural Dynamics*, 36, 2059–2079.

[23] Padgett JE, Nielson BG, DesRoches R (2008): Selection of optimal intensity measures in probabilistic seismic demand models of highway bridge portfolios. *Earthquake Engineering and Structural Dynamics*, 37, 711–725.

[24] Tothong P, Luco N (2007): Probabilistic seismic demand analysis using advanced ground motion intensity measures. *Earthquake Engineering and Structural Dynamics*, 36, 1837–1860.

[25] Giovenale P, Cornell AC, Esteva L (2004): Comparing the adequacy of alternative ground motion intensity measures for the estimation of structural responses. *Earthquake Engineering and Structural Dynamics*, 33,951–979.

[26] Cervenka J, Chandra JM, Saouma V (1998): Mixed Mode Fracture of Cementitious Bimaterial Interfaces; Part II: Numerical Simulation. *Engineering Fracture Mechanics*, 60(1), 95–107.

[27] Saouma V, Cervenka J, Reich R: Merlin Finite Element User's Manual http://civil.colorado.edu/~saouma/pdf/Software/users.pdf2010.

[28] Hariri-Ardebili MA, Saouma VE (2016): Collapse Fragility Curves for Concrete Dams: Comprehensive Study. *ASCE Journal of Structural Engineering*, 142(10), 04016075.

